

Raman scattering study of wurtzite and rocksalt InN under high pressure

C. Pinquier, F. Demangeot, and J. Frandon

Laboratoire de Physique des Solides, CNRS-UMR 5477, IRSAMC, Université Paul Sabatier, 118 route de Narbonne, 31062 Toulouse Cedex 4, France

J.-C. Chervin, A. Polian, B. Couzinet, and P. Munsch

Physique des Milieux Denses, IMPMC, CNRS-UMR 7590, Université Pierre et Marie Curie, 140 rue de Lourmel, 75015 Paris, France

O. Briot, S. Ruffenach, B. Gil, and B. Maleyre

Groupe d'Etude des Semiconducteurs, Université Montpellier II, Case Courrier 074, 34095 Montpellier Cedex 5, France

(Received 9 January 2006; revised manuscript received 15 February 2006; published 30 March 2006)

Indium nitride under high pressure (up to 50 GPa) was analyzed by means of Raman spectroscopy. The wurtzite to rocksalt phase transition was evidenced at the pressure of 13.5 ± 0.5 GPa and the pressure dependence of vibration modes of both structures was investigated, leading to the determination of linear pressure coefficients and mode Grüneisen parameters. Influence of the pressure dependence of the energy gap on the spectra intensity is also discussed.

DOI: [10.1103/PhysRevB.73.115211](https://doi.org/10.1103/PhysRevB.73.115211)

PACS number(s): 61.50.Ks, 63.20.-e

I. INTRODUCTION

Group-III nitrides have been widely investigated because of their promising applications for optoelectronic devices. Indium nitride was the least studied as it is rather difficult to grow high quality material, and particularly to elaborate thick undoped layers. This material has known increased interest thanks to recent progress in growth techniques; nevertheless, to date, the knowledge of InN properties remains quite poor. InN films are usually grown on various buffer layers and substrates, and so, are generally strained due to the significant lattice mismatch and the difference in thermal expansion between the film and the underlying layer. Raman spectroscopy can be employed to probe the strain fields: for this purpose, deformation potentials are key parameters. While they have been extensively studied in the case of GaN (Refs. 1–3) and AlN,^{4,5} only one report can be found for InN.⁶ However, in the last reference, owing to the lack of experimental data, calculated mode Grüneisen parameters⁷ were used. The experimental evaluation of the latter requires high-pressure measurements.

In a previous paper on Raman scattering in wurtzite InN under hydrostatic pressure,⁸ up to 13.2 GPa, we evidenced the beginning of the wurtzite to rocksalt phase transition and analyzed the long-wavelength E_2 and $A_1(\text{LO})$ phonons relative to the wurtzite structure. Here, higher pressure experiments (up to 50 GPa) are reported: the phase transition was achieved and the Raman signal of rocksalt InN is discussed. Linear pressure coefficients and mode Grüneisen parameters are determined, not only for the wurtzite E_2 and $A_1(\text{LO})$ phonons, but also for the $A_1(\text{TO})$ phonon, as well as the rocksalt modes. Moreover, the study is completed by quantitative results on Raman signal intensities.

II. EXPERIMENTAL DETAILS

The sample under study is a 1.4- μm -thick wurtzite InN film, directly deposited on a sapphire substrate by metalor-

ganic vapor phase epitaxy (MOVPE).⁹ The doping level determined by Hall measurements is $2.3 \times 10^{19} \text{ cm}^{-3}$, which is typical for such layers.¹⁰ Due to the large lattice mismatch of 26% between the two materials, InN could be easily detached from the substrate, thus producing free-standing flakes of $\sim 20 \mu\text{m}$ in size.

Pressure experiments were conducted using a membrane diamond anvil cell (DAC).¹¹ The culets of the anvils were 400 μm in diameter. The pressure transmitting medium was argon, loaded at high pressure by an optically monitored method.¹² The stainless steel gasket was preindented to a thickness of approximately 40 μm , and the hole forming the experimental volume had a diameter of 160 μm , just after loading, as shown in the inset of Fig. 1. The pressure values (up to 50 GPa) were determined by the ruby fluorescence method.^{13,14} The accuracy of this measurement (± 0.1 GPa) is limited by pressure heterogeneity inside the DAC, which cannot be neglected for the highest pressures.¹⁵

Spectra of InN Raman scattering and ruby luminescence were recorded in backscattering geometry by means of a HR 460 Raman spectrometer with a holographic notch filter and a charge coupled device (CCD) camera, and equipped with a microscope. The 2.41 eV (514.5 nm) Ar^+ line was used for excitation. Acquisition time ranged between 300 and 900 s. Then, all spectra were normalized in time or to the integrated area, as explained later.

III. RESULTS AND DISCUSSION

Raman spectra (normalized in time) under increasing pressure up to 14.1 GPa are displayed in Fig. 1. The luminescence at high frequency is due to the diamond anvils, as well as the peak at 760 cm^{-1} , marked with an asterisk, which corresponds to the diamond 2TA phonon. The modes respectively observed at 440, 491, and 592 cm^{-1} at atmospheric pressure are attributed to the phonons of InN, namely $A_1(\text{TO})$, long-wavelength E_2 , and $A_1(\text{LO})$, in agreement with

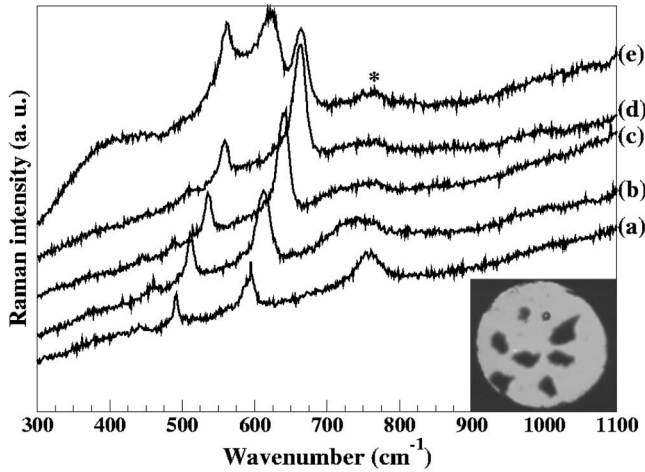


FIG. 1. Raman spectra of wurtzite InN under increasing pressure. The values of the pressure are respectively: (a) 0.3, (b) 3.5, (c) 7.7, (d) 12.5, and (e) 14.1 GPa. The asterisk marks the 2TA mode of the diamond. In the inset: photograph of the experimental volume in the DAC loaded with argon, exhibiting InN flakes (in black) and the ruby sphere (the smallest piece, at the top of the picture).

the selection rules relative to wurtzite crystals in backscattering geometry. The TO phonon does not exhibit a strong intensity: it is forbidden on the surface of the sample and allowed on the edge only. Actually, the orientation of InN flakes cannot be monitored inside the DAC. As a consequence, the incident photon wave vector is not strictly perpendicular to the surface of the sample, allowing the activation of the TO mode. Moreover, despite the high free carrier concentration, the LO mode does not couple with the plasmon as commonly expected.¹⁶ Such a behavior has already been observed in highly doped InN (Refs. 17 and 18) and was interpreted as the breakdown of the wave vector conservation.^{19,20} Thus, for sake of simplicity, we will call the wurtzite modes TO, E_2 , and LO.

Phonon frequencies increase with pressure. As illustrated in the left part of Fig. 2 for the three observed wurtzite phonons, the frequency evolution can be fitted linearly by the equation

$$\omega_i = \omega_{i0} + a_i p, \quad (1)$$

where ω_{i0} is the frequency of the i th phonon at zero pressure, p is the pressure, and $a_i = (\partial\omega_i / \partial p)_{p=0}$ is the linear pressure coefficient for the given mode. Then, the i th mode Grüneisen parameter is deduced using the relation^{21,22}

$$\gamma_i = - \frac{\partial \ln \omega_i}{\partial \ln V} = \frac{B_0}{\omega_{i0}} a_i, \quad (2)$$

where the bulk modulus B_0 is defined as the inverse of the isothermal compressibility. Several theoretical studies were attempted to determine the bulk modulus,^{7,23–28} leading to values ranging between 116 and 146 GPa, which are lower than those for GaN and AlN. On the contrary, only very few experimental determinations were performed,^{30,31} using x-ray diffraction. For example, the value obtained by Ueno *et al.*³¹ is $B_0 = 125.5$ GPa.

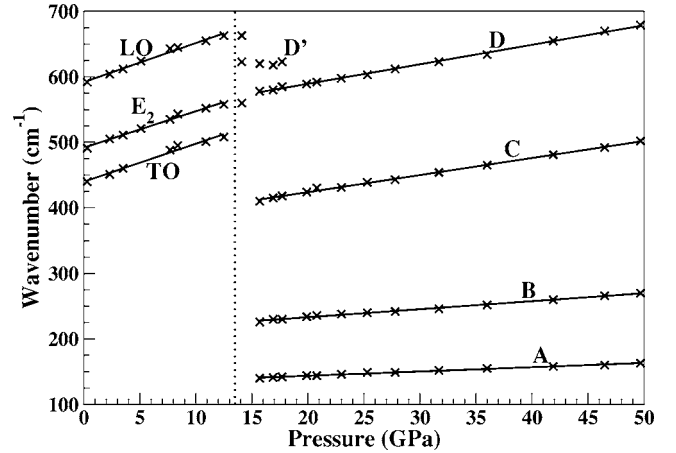


FIG. 2. InN mode wave numbers vs pressure at the upstroke. Crosses represent experimental measurements, fitted by linear regressions (solid lines) for the TO, E_2 , and LO phonons of the wurtzite phase, and for the A, B, C, and D modes of the rocksalt structure (see Fig. 3). The dotted line symbolizes the phase transition pressure of 13.5 GPa.

Grüneisen parameters calculated for the three phonons observed in the wurtzite phase of InN, with the latter experimental value of B_0 , are given in Table I. The results for the E_2 and LO modes are in very good agreement with our previous determination,⁸ which was obtained with another experimental setup: indeed, the ratios $\frac{\gamma_i}{B_0} = \frac{a_i}{\omega_{i0}}$ are very similar in both studies for these two phonons. However, different references were chosen for the bulk modulus, which explains the slight discrepancy in the values of the calculated mode Grüneisen parameters. Moreover, the TO phonon was not observed in our previous study.⁸

At pressures above 13.5 GPa, the Raman spectra drastically change, as displayed in Fig. 3. The phonons of the wurtzite structure vanish while new modes appear and the whole signal appreciably increases. The new modes are labeled A, B, C, D, and D' , as defined in Fig. 3; when pressure increases, the D' mode merges into D. Such a behavior is characteristic of the expected wurtzite (hexagonal) to rock-

TABLE I. Results of linear regressions (ω_{i0} and a_i) and calculated mode Grüneisen parameters γ_i , using 125.5 and 170 GPa for the bulk modulus of wurtzite and rocksalt InN, respectively.

| Vibration mode i | ω_{i0} (cm ⁻¹) | a_i (cm ⁻¹ GPa ⁻¹) | γ_i |
|--------------------|-----------------------------------|---|------------|
| Wurtzite | | | |
| TO | 439.7 | 5.81 | 1.66 |
| E_2 | 491.7 | 5.56 | 1.42 |
| LO | 591.9 | 5.96 | 1.26 |
| Rocksalt | | | |
| A | 130.7 | 0.65 | 0.85 |
| B | 208.8 | 1.22 | 0.99 |
| C | 371.7 | 2.61 | 1.19 |
| D | 529.8 | 2.98 | 0.96 |

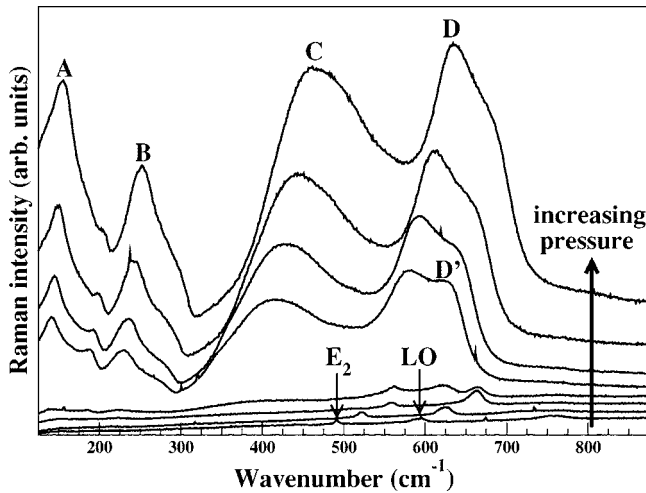


FIG. 3. Raman spectra of InN under high pressure at the up-stroke. Pressure values are respectively: 0.3, 5.1, 12.5, 14.1, 16.9, 20.8, 27.8, and 36.0 GPa. At higher pressures, up to 50 GPa, the general shape of spectra does not evolve anymore. Wurtzite phonons E_2 and LO are indicated by arrows; the modes labeled A, B, C, D, and D' are relative to the rocksalt structure.

salt (cubic) phase transition, and the transition pressure is determined to be 13.5 ± 0.5 GPa, in agreement with theoretical and experimental values found in the literature.^{8,26,28,29,31–34} The accuracy of the latter value is mainly limited by the pressure sweep. The spectrum (e) in Fig. 1, acquired at 14.1 GPa, simultaneously evidences wurtzite and rocksalt modes, attesting the coexistence of both phases. Consequently, the transition does not occur instantaneously at the time scale of our Raman measurements.

This kind of behavior was already mentioned in the case of InN (Refs. 31 and 33) and interpreted by Bellaiche *et al.*³³ in terms of gradual transition which could be driven by second-neighbor interactions between indium atoms. According to this theoretical study, a second-order isostructural phase transition occurs in the same pressure range as the hexagonal to cubic first-order transition. As a result, InN should transform into an intermediate structure and, within a pressure interval of a few gigapascals, both phases coexist before the transition is completed. The comparison of the possible mechanisms involved in the wurtzite to rocksalt high pressure transition seems to be in agreement with such an interpretation. Indeed, the transition can mainly proceed by two paths: through a continuous deformation implying an hypothetical hexagonal intermediate phase, referred to as *h*-MgO, or through a tetragonal path. Both mechanisms were theoretically studied in GaN (Ref. 35) and ZnO,²⁹ respectively. Saitta *et al.*²⁹ predicted the InN phase transition to occur according to the tetragonal way, and gave the evidence that this transformation is related to second-neighbor interactions, which is in agreement with the previous interpretation³³ in terms of gradual transition.

Actually, first-order Raman scattering is forbidden by the selection rules in the case of the rocksalt structure, and thus the phase transition should be accompanied by the disappearance of the Raman signal, as reported for other materials.^{36,37} To explain the strong signal observed beyond the transition,

disorder activated scattering from the phonon density of states (DOS) can be put forward, as already invoked in the case of GaN. Indeed, Halsall *et al.*³⁸ studied the GaN wurtzite to rocksalt phase transition by comparing experimental Raman spectra acquired under high pressure with *ab initio* calculations. The conclusion was that the Raman signal assigned to the cubic structure was associated to scattering by the DOS. The phase transition was supposed to occur instantaneously on a local scale, leading to a very high degree of local disorder at the origin of the disorder activation of the phonon DOS scattering. The same behavior can be expected for InN. Unfortunately, the only DOS calculations for rocksalt InN were achieved at zero pressure.³⁹

Some Raman spectra were also recorded in backscattering geometry on the edge of the sample (not shown): at pressures lower than the pressure phase transition, the wurtzite E_2 mode was absent, attesting that the experimental geometry was $X(ZZ)\bar{X}$ in Porto notation. Above the phase transition, spectra acquired on the edge and on the surface of the sample were similar, highlighting that rocksalt vibrational modes are not sensitive to light polarization. This is a further argument in favor of the DOS scattering model. Consequently, we will assign the vibrational modes of the rocksalt structure to the DOS scattering.

The rocksalt mode frequencies increase with pressure. This behavior, shown in the right part of Fig. 2, can be modeled by a linear law, as previously done for the wurtzite phonons. Linear pressure coefficients were calculated according to Eq. (1) and given in Table I. Modes in the rocksalt high pressure phase clearly appear to be less sensitive to pressure than those in the low pressure wurtzite structure.

Mode Grüneisen parameters are deduced from Eq. (2). The bulk modulus of rocksalt InN was experimentally determined to be 170 GPa by Uehara *et al.*³² which is in the range of the calculated values.^{23,26,40} Like the other nitrides,³² InN exhibit a remarkably large bulk modulus when crystallized in the rocksalt structure. Modes Grüneisen parameters displayed in Table I were calculated using the latter value. Note their particularly low values, due to the extremely low values of pressure coefficients.

We also analyzed the Raman signal intensities. In order to make a quantitative study, diamond luminescence was subtracted and the integrated intensity of the entire spectra was normalized. As shown in the inset in Fig. 4, the phase transition is accompanied by a large increase of the scattered signal on the whole, suggesting an important change of the absorption beyond the phase transition: indeed, if the penetration depth is higher, the probed volume increases, and so does the Raman signal. Nevertheless, no experimental data were found in the literature about rocksalt InN absorption in order to check such an assumption. Further experiments are actually in progress to elucidate this point.

Moreover, intensity of each InN mode is plotted versus pressure in the same figure. Concerning the wurtzite structure, the LO phonon is significantly more enhanced than the non polar mode: although both phonons exhibit similar intensity at zero pressure, the intensity ratio of the two modes is larger than two when hydrostatic pressure reaches 10 GPa. This could be explained by a resonance effect. Indeed, room

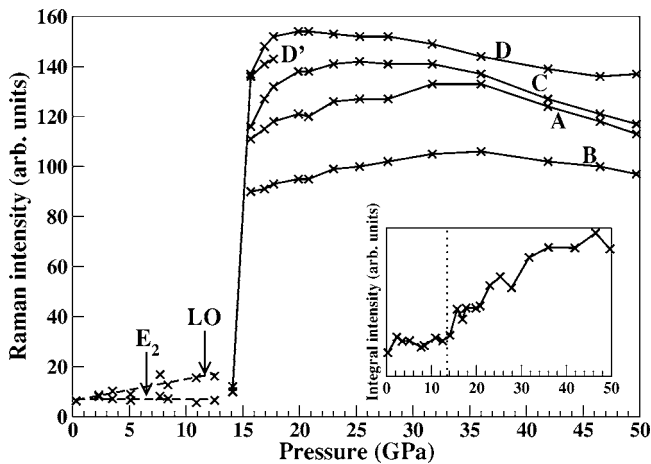


FIG. 4. InN mode intensities (arbitrary scale) vs pressure. Dashed lines correspond to linear regressions for wurtzite phonon intensity. The rocksalt modes, labeled A, B, C, D, and D', are defined in Fig. 3. In inset: integral intensity of the whole spectra vs pressure; the dotted line symbolizes the phase transition pressure of 13.5 GPa.

temperature photoluminescence experiments were made using the 2.41 eV excitation line at atmospheric pressure (not shown): a strong emission signal is found at 1.62 eV, as well as multi-LO phonon scattering, what gives the evidence that Fröhlich mechanism is partly involved in the scattering process. This result agrees well with previous resonant Raman scattering measurements.^{18,41} Kuball *et al.*¹⁸ suggest the presence of a critical point in the InN electronic band structure within 200–300 meV of 1.49 eV leading to the enhancement of the LO mode when excitation energy decreases. As in the previous reference,¹⁸ no assumption is made on the involved

electronic states; in particular, resonance effects are not associated with the InN band gap, which remains controversial. Anyway, all the bands are expected to increase with pressure and we can reasonably assume that they are up-shifted with pressure coefficients of the same order of magnitude. Li *et al.*⁴² determined the pressure coefficient of the band gap to be 3 meV/kbar. Thus we expect a blueshift of ~ 0.3 eV of all the bands when hydrostatic pressure increases up to 10 GPa: the luminescence energy should increase, and so, lie closer to the excitation line at the pressure upstroke. By this way, Fröhlich scattering mechanism should be promoted and the LO phonon favored with respect to the E_2 mode.

After reaching the maximum pressure of approximately 50 GPa, about ten spectra were acquired at the downstroke (not shown), and we typically waited several hours between two successive acquisitions. A clear hysteresis effect was observed: at pressures lower than 14.1 GPa, rocksalt modes still appeared, attesting a delay in the reverse phase transition. This behavior has already been experimentally pointed out for InN under high pressure, with energy dispersive x-ray diffraction³⁴ and Raman scattering.⁸ Nevertheless, InN cubic to hexagonal backtransformation occurs. The transition is fully reversible and no amorphization effect was evidenced.

IV. CONCLUSION

In summary, vibration modes of InN were investigated under high pressure, up to 50 GPa, by means of Raman scattering. The high pressure transition from wurtzite to rocksalt structure was evidenced at a pressure of 13.5 ± 0.5 GPa. These experiments allowed us to determine linear pressure coefficients and mode Grüneisen parameters for modes of both phases. By coupling these results with x-ray diffraction measurements of biaxially strained InN layers, deformation potentials of phonons could be evaluated. Raman signal intensities were also discussed.

¹F. Demangeot, J. Frandon, P. Baules, F. Natali, F. Semond, and J. Massies, *Phys. Rev. B* **69**, 155215 (2004).

²F. Demangeot, J. Frandon, M. A. Renucci, O. Briot, B. Gil, and R. L. Aulombard, *Solid State Commun.* **100**, 207 (1996).

³V. Yu. Davydov, N. S. Averkiev, I. N. Goncharuk, D. K. Nelson, I. P. Nikitina, A. S. Polkovnikov, A. N. Smirnov, M. A. Jacobson, and O. K. Semchinova, *J. Appl. Phys.* **82**, 5097 (1997).

⁴J. Gleize, M. A. Renucci, J. Frandon, E. Bellet-Amalric, and B. Daudin, *J. Appl. Phys.* **93**, 2065 (2003).

⁵A. Sarua, M. Kuball, and J. E. Van Nostrand, *Appl. Phys. Lett.* **81**, 1426 (2002).

⁶V. Darakchieva, P. P. Paskov, E. Valcheva, T. Paskova, B. Monemar, M. Schubert, H. Lu, and W. J. Schaff, *Appl. Phys. Lett.* **84**, 3636 (2004).

⁷K. Kim, W. R. L. Lambrecht, and B. Segall, *Phys. Rev. B* **53**, 16310 (1996).

⁸C. Pinquier, F. Demangeot, J. Frandon, J. W. Pomeroy, M. Kuball, H. Hubel, N. W. A. van Uden, D. J. Dunstan, O. Briot, B. Maleyre, S. Ruffenach, and B. Gil, *Phys. Rev. B* **70**, 113202 (2004).

⁹B. Maleyre, O. Briot, and S. Ruffenach, *J. Cryst. Growth* **269**, 15

(2004).

¹⁰A. G. Bhuiyan, A. Hashimoto, and A. Yamamoto, *J. Appl. Phys.* **94**, 2779 (2003).

¹¹R. Le Toullec, J. P. Pinceaux, and P. Loubeyre, *High Press. Res.* **1**, 77 (1988).

¹²B. Couzinet, N. Dahan, G. Hamel, and J.-C. Chervin, *High Press. Res.* **23**, 409 (2003).

¹³H. K. Mao, P. M. Bell, J. W. Shaner, and D. J. Steinberg, *J. Appl. Phys.* **49**, 3276 (1978).

¹⁴J.-C. Chervin, B. Canny, and M. Mancinelli, *High Press. Res.* **21**, 305 (2001).

¹⁵J.-C. Chervin, C. Power, and A. Polian, *High Press. Res.* **25**, 97 (2005).

¹⁶A. Kasic, M. Schubert, Y. Saito, Y. Nanishi, and G. Wagner, *Phys. Rev. B* **65**, 115206 (2002).

¹⁷T. Inushima, M. Higashiwaki, and T. Matsui, *Phys. Rev. B* **68**, 235204 (2003).

¹⁸M. Kuball, J. W. Pomeroy, M. Wintrebert-Fouquet, K. S. A. Butcher, H. Lu, and W. J. Schaff, *J. Cryst. Growth* **269**, 59 (2004).

¹⁹F. Demangeot, C. Pinquier, J. Frandon, M. Gaio, O. Briot, B.

- Maleyre, S. Ruffenach, and B. Gil, *Phys. Rev. B* **71**, 104305 (2005).
- ²⁰J. S. Thakur, D. Haddad, V. M. Naik, R. Naik, G. W. Auner, H. Lu, and W. J. Schaff, *Phys. Rev. B* **71**, 115203 (2005).
- ²¹M. Blackman, *Proc. Phys. Soc. London, Sect. B* **70**, 827 (1957).
- ²²W. B. Daniels, in *Lattice Dynamics*, edited by R. F. Wallis (Pergamon Press, Oxford, 1965), p. 273.
- ²³N. E. Christensen and I. Gorczyca, *Phys. Rev. B* **50**, 4397 (1994).
- ²⁴A. F. Wright and J. S. Nelson, *Phys. Rev. B* **51**, 7866 (1995).
- ²⁵C. Stampfl and C. G. Van de Walle, *Phys. Rev. B* **59**, 5521 (1999).
- ²⁶J. Serrano, A. Rubio, E. Hernández, A. Muñoz, and A. Mujica, *Phys. Rev. B* **62**, 16612 (2000).
- ²⁷N. Farrer and L. Bellaïche, *Phys. Rev. B* **66**, 201203(R) (2002).
- ²⁸L. Mancera, J. A. Rodríguez, and N. Takeuchi, *Phys. Status Solidi B* **241**, 2424 (2004).
- ²⁹A. M. Saitta and F. Decremps, *Phys. Rev. B* **70**, 035214 (2004).
- ³⁰A. U. Sheleg and V. A. Savastenko, *Inorg. Mater.* **15**, 1257 (1979).
- ³¹M. Ueno, M. Yoshida, A. Onodera, O. Shimomura, and K. Takemura, *Phys. Rev. B* **49**, 14 (1994).
- ³²S. Uehara, T. Masamoto, A. Onodera, M. Ueno, O. Shimomura, and K. Takemura, *J. Phys. Chem. Solids* **58**, 2093 (1997).
- ³³L. Bellaïche, K. Kunc, and J. M. Besson, *Phys. Rev. B* **54**, 8945 (1996).
- ³⁴Q. Xia, H. Xia, and A. L. Ruoff, *Mod. Phys. Lett. B* **8**, 345 (1994).
- ³⁵S. Limpijumngong and W. R. L. Lambrecht, *Phys. Rev. Lett.* **86**, 91 (2001).
- ³⁶P. T. C. Freire, M. A. Araújo Silva, V. C. S. Reynoso, A. R. Vaz, and V. Lemos, *Phys. Rev. B* **55**, 6743 (1997).
- ³⁷P. Perlin, C. Jauberthie-Carillon, J. P. Itie, A. San Miguel, I. Grzegory, and A. Polian, *Phys. Rev. B* **45**, 83 (1992).
- ³⁸M. P. Halsall, P. Harmer, P. J. Parbrook, and S. J. Henley, *Phys. Rev. B* **69**, 235207 (2004).
- ³⁹G. Kaczmarczyk, A. Kaschner, S. Reich, A. Hoffmann, C. Thomsen, D. J. As, A. P. Lima, D. Schikora, K. Lischka, R. Averbeck, and H. Riechert, *Appl. Phys. Lett.* **76**, 2122 (2000).
- ⁴⁰A. Muñoz and K. Kunc, *J. Phys.: Condens. Matter* **5**, 6015 (1993).
- ⁴¹V. M. Naik, R. Naik, D. B. Haddad, J. S. Thakur, G. W. Auner, H. Lu, and W. J. Schaff, *Appl. Phys. Lett.* **86**, 201913 (2005).
- ⁴²S. X. Li, J. Wu, E. E. Haller, W. Walukiewicz, W. Shan, H. Lu, and W. J. Schaff, *Appl. Phys. Lett.* **83**, 4963 (2004).